International Journal of Thermophysics, Vol. 16, No. 1, 1995

Layer-by-Layer Transitions in Liquid Crystals[1]

T. Stoebe,[2] A. J. Jin,[2] P. Mach,[2] and C. C. Huang[2,3]

Employing our free-standing film calorimetric system, we have identified three remarkable layer-by-layer transitions in several liquid crystal compounds. Each of these transitions can be well described by the simple power-law form: $L = L_0 t^{-\nu}$. The layering transitions found near the smectic-A–hexatic-B and smectic-A–crystal-B transitions are well characterized by the exponent $\nu \approx 1/3$. This value is consistent with models based on a van der Waals-like dominant intermolecular interaction. Another novel layer-by-layer thinning transition has been discovered above the bulk smectic-A isotropic transition of a perfluorinated liquid crystal compound. The value of the exponent obtained, $\nu \approx 3/4$, cannot be easily explained using familiar models.

KEY WORDS: free-standing film; heat capacity; layer-by-layer transition; liquid crystal; smectic-A–hexatic-B transition.

1. INTRODUCTION

Liquid crystals are organic molecules, anisotropic in shape, which display one or more mesophases between the crystalline state and the isotropic liquid. An important class of these mesophases is the smectic phases [derived from the Greek $\sigma\mu\eta\gamma\mu\alpha$ (=soap)]. The smectic phases exist as layered structures in which the interlayer interaction is relatively weak. Because the layers are not coupled strongly, interesting surface effects can be apparent and the phase behavior of liquid crystals is strongly influenced by the proximity of interfaces. For example, the liquid crystal/vapor interface has proven to be extremely rich and has exhibited various intriguing physical phenomena. Furthermore, the interaction between the liquid crystal and

[1] Paper presented at the Twelfth Symposium on Thermophysical Properties, June 19–24, 1994, Boulder, Colorado, U.S.A.

[2] School of Physics and Astronomy, University of Minnesota, Minneapolis, Minnesota 55455, U.S.A.

[3] To whom correspondence should be addressed.

0195-928X/95/0100-0033$07.50/0 © 1995 Plenum Publishing Corporation

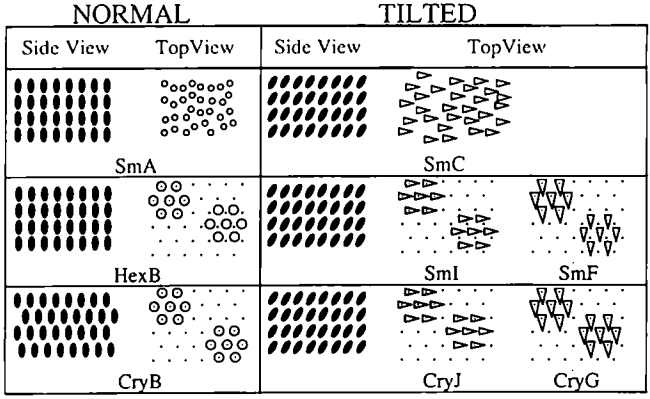

Fig. 1. Schematic illustration of the molecular arrangements in eight liquid crystal mesophases.

the substrate plays a vital role in the proper function of liquid-crystal displays and is currently of great interest in industry.

A schematic illustration of the molecular arrangement in the relevant smectic phases is shown in Fig. 1. The smectic-A (SmA) and smectic-C (SmC) phases exhibit simply liquid-like molecular arrangement within the planes of the layers. Because the hexatic-B (HexB), smectic-I (SmI), and smectic-F (SmF) phases possess long-range bond-orientational order, they can be distinguished from the less ordered SmA and SmC phases. However, unlike truly crystalline phases, these "hexatic" phases do not possess long-range positional order. The remaining phases, i.e., crystal-B (CryB), crystal-J (CryJ), and crystal-G (CryG), do, in fact, exhibit long-range positional order and are crystalline. The molecules are free to rotate about their long axes in each of the phases included in Fig. 1. In the normal phases (SmA, HexB, and CryB), the molecular long axes are parallel to the layer normal. The tilted phases exhibit a finite angle between the layer normal and the molecular long axes.

Much like a soap film on a ring, free-standing smectic liquid-crystal films can be prepared and suspended over a hole cut into a film plate. These substrate-free films constitute an amazing physical system. Provided the appropriate compounds are chosen, the sample thickness can often be varied from two to a few hundred molecular layers (≈ 50 Å to $\approx 1\,\mu$m) in a matter of seconds by simply spreading new films until the desired thickness is obtained. A number of interesting experiments [1] (e.g., calorimetric investigations, electron and X-ray diffraction, light-scattering, mechanical measurements, optical observations, optical reflectivity, etc.) have been conducted on free-standing liquid-crystal film systems to

investigate inter- and intralayer molecular order, the evolution of phase transitions as the system is taken from the thick-film to the thin-film limit, and substrate-free two-dimensional transitions and the effect of free surfaces.

The atoms or molecules at the surfaces of the vast majority of bulk solids are in a somewhat less ordered state than those in the interior. As a result, the melting process usually begins at the surface and progresses inward as the transition is approached from below. Unlike the situation in conventional solids, the surface tension associated with the vapor/liquid crystal interface tends to promote order near the surface of the liquid-crystal sample. This effectively increases the surface transition temperature. Consequently, ordering transitions tend to start at the vapor/liquid crystal interface and proceed inward as the transition is approached from above. Due to the relatively weak interlayer interaction and the smoothness of the "substrate," such preferential surface ordering generally results in the transition progressing in a layer-by-layer fashion.

A layering transition involving smectic liquid crystals was first demonstrated by Ocko et al. [2]. In their experimental investigation, they measured the angular dependence of the X-ray specular reflectivity from the liquid-crystal free surface as a function of temperature above the bulk smectic-A–isotropic transition of 12CB (dodecylcyanobiphenyl). The reflectivity data can be described in terms of a sinusoidal density modulation, starting at the surface and terminating abruptly after an integral number of layers. The data are therefore consistent with the discrete penetration of the bulk isotropic phase by an increasing number of SmA bilayers as the temperature is reduced. Employing computer-enhanced polarized video microscopy, Swanson et al. [3] studied the layer-by-layer surface ordering transition of free-standing films of 4-(*n*-nonyloxy) benzylidene-4-(*n*-butyl) aniline (90.4). The remarkable resolution of this optical technique enabled them to resolve 28 separate layering transitions. The transition temperatures of the first 10 layers were found to be well described by the simple power-law form, $L = L_0 t^{-\nu}$. The fitting of the data produced the exponent $\nu = 0.37$, indicating that a van der Waals-type interaction [4] dominates the interlayer coupling and is responsible for the layering transition.

2. RESULTS AND DISCUSSION

In order to perform a crucial experimental test of the ability of the novel two-dimensional melting theory to describe the SmA–HexB transition in liquid crystals, we have established a state-of-the-art AC differential calorimetric system [5, 6]. The system is now capable of simultaneous measurement of both heat capacity and optical reflectivity of free-standing films only two molecular layers in thickness. *The resolution of both probes*

is better than a few parts in 10^5. The fact that two-layer films exhibit only a single heat-capacity anomaly, while thicker films display more than one peak associated with the SmA–HexB transition in the *nm*OBC compounds, supports the conclusion that two-layer films possess two-dimensional (2D) thermodynamic behavior. The label, *nm*OBC, refers to members of the *n-alkyl*-4′-*n-alk*oxybiphenyl-4-carboxylate homologous series. Our calorimetric and optical reflectivity data on two-layer films indicate that the 2D melting theory is not sufficient to describe the nature of the SmA–HexB transition. Because previous high-resolution X-ray and electron beam diffraction data convincingly demonstrate the existence of bond-orientational order in the HexB phase, the concept of hexatic order is clearly important to our understanding of this transition. However, since our data cannot be described simply in terms of a disclination unbinding transition, additional molecular order (e.g., herringbone order) must also be established through the SmA–HexB transition [6].

Because two-layer films appear to be two-dimensional, they are prohibited from undergoing a series of transitions dependent on depth into the film. Surprisingly, however, even films just three molecular layers thick do exhibit distinct anomalies corresponding to separate transitions in the surface and interior layers. Upon cooling these thicker *nm*OBC films, the SmA–HexB transition has been observed to originate at the outermost surface layers and progress into the film in a layer-by-layer fashion [7]. Among the nine *nm*OBC compounds that exhibit the SmA–HexB transition, 3(10)OBC possesses the longest total alkyl chain length. The increased separation between the biphenyl cores may further reduce the interlayer coupling. Such reduced coupling is consistent with the observation that 3(10)OBC not only exhibits the most pronounced heat-capacity peaks but also displays up to five (rather than four) separate heat-capacity anomalies near the SmA–HexB transition for sufficiently thick films [7]. Figure 2 displays the temperature dependence of the heat capacity associated with the SmA–HexB transition in (a) 60-, (b) 30-, and (c) 6-layer 3(10)OBC free-standing films. For clarity, the temperature axes are expanded in the insets in Figs. 2a and b, to make the layer transitions more apparent near the large interior anomalies. Despite the impressive resolution of the calorimetric measurements ($S/N \approx 1 \times 10^5$), we are unable to resolve additional heat-capacity peaks. It is therefore unclear whether the transition continues in a layer-by-layer fashion throughout the film (complete wetting) or is terminated by a single bulk transition involving the rest of the interior layers (incomplete wetting).

The behavior exhibited in Fig. 2 is highly unusual. Previous to this work, layer-by-layer transitions had been theoretically addressed and/or experimentally investigated only in systems exhibiting a first-order

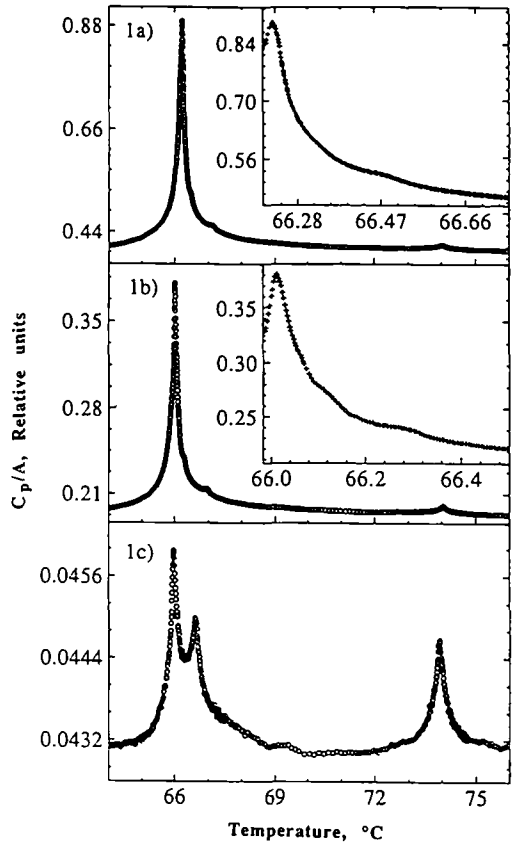

Fig. 2. Temperature variation of heat capacity for (a) 60-, (b) 30-, and (c) 6-layer 3(10)OBC free-standing films near the SmA–HexB transition. To make the layer transition more apparent near the large interior anomaly, the temperature axis is expanded in the insets.

transition [4]. However, none of the heat-capacity anomalies in Fig. 2 exhibit measurable (<5-mK) thermal hysteresis [6, 8]. Moreover, the well-separated anomalies can be successfully fit to a simple power law [9]. These two points are strongly indicative of the continuous nature of these transitions. Thus the observed layer-by-layer transition strongly suggests that there should not have been interlayer coupling for the establishment of the hexatic order. In principle, the predicted divergence of the order-parameter susceptibility (χ) makes the discussion of a layer-by-layer transition near a continuous transition appear unrealistic. However, the somewhat flexible alkyl chains may act effectively to screen the hexatic

interaction while allowing the smectic phases to maintain their layer structure. The layers therefore act as barriers to the hexatic fluctuations along the film normal and allow the transition to progress in a series of discrete steps.

The ordering effects of the surface tension inherent in the liquid crystal/vapor interface have been clearly demonstrated by an X-ray diffraction study [10]. The authors found that the molecular fluctuation amplitudes increased sharply as a function of increasing depth into the film, strongly supporting the hypothesis that the ordering originates at the free surfaces. Furthermore, this study suggests that there may be a variation of in-plane molecular density $[\rho_A(L)]$ between the outermost layers and the interior. Because the SmA–HexB transition can probably also be density driven, it is reasonable to assume the transition temperature of each molecular layer to be a function of $\rho_A(L)$. The outermost layers, having the highest density due to the surface tension, would possess the highest transition temperature and the transition would progress inward upon decreasing temperature. Unfortunately, despite the high resolution of our optical reflectivity probe (which is sensitive to the index of refraction and, hence, density), we have not yet succeeded in measuring any variation of the in-plane density as a function of film thickness. The transition temperatures may be strongly dependent on small changes of the in-plane density, however, and this failure does not greatly weaken the above argument.

The temperatures of the individual layer transitions can be measured with a high resolution and denoted $T_c(L)$, where L gives the separation (measured in units of layers) between the nearest film/vapor interface and the layer in question. The temperature dependence of the penetration depth (L versus $[T_c(L) - T_c]/T_c$, where T_c is the bulk transition temperature) of the surface ordering transitions is shown in Fig. 3 for the three films introduced in Fig. 2. The data can be fitted to the simple power-law form: $L = L_0\ ([T_c(L) - T_c]/T_c)^{-\nu}$, yielding values for the exponent $\nu = 0.32 \pm 0.01$ and coefficient $L_0 = 0.30$. As shown below, these results indicate that the interlayer interaction is dominated by van der Waals-like forces [4]. It is also interesting to note that the interlayer interaction does not change significantly over the range of film thickness studied.

The transition temperature data can be analyzed in terms of standard wetting calculations [11]. The surface HexB phase appears well above the maximum stable temperature of the bulk HexB phase. The system free energy must therefore be significantly reduced by replacing the SmA–vapor interfacial coefficient (γ_{AV}) with the sum of the SmA–HexB and HexB–vapor interfacial coefficients ($\gamma_{AB} + \gamma_{BV}$). However, if, as in this case, the thickness of the surface phase is not macroscopically large, the mean-field

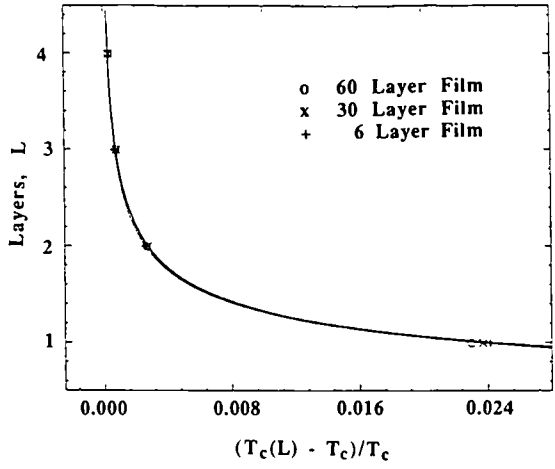

Fig. 3. Plot of L vs $[T_c(L) - T_c]/T_c$ of the layer transition temperature, $T_c(L)$, obtained from Fig. 2. The solid line is the fit to the power-law expression.

free energy reduction per unit area (denoted here as δF_1) will be a function of L due to the truncation of the interactions across the interfaces. For power-law forces between interfaces varying as (1/distance)^p, this free energy contribution is given by

$$\delta F_1 = \Delta\gamma(1 - aL^{1-p}) \tag{1}$$

where $\Delta\gamma = \gamma_{AV} - \gamma_{AB} - \gamma_{BV}$ and coefficient a is a constant of order unity. This free energy reduction competes with the free energy increase due to the lower entropy of the surface HexB phase. This increase in free energy is clearly related to the volume of the HexB phase and this term (denoted here δF_2) must be simply proportional to the thickness, L, after dividing by the unit area. Because the SmA and HexB phases have the same free-energy density at the bulk transition temperature (T_c), $\delta F_2 = 0$ at T_c. However, for $T > T_c$, δF_2 can be expanded in terms of $t = (T - T_c)/T_c$. To lowest order, δF_2 may be expressed as $\delta F_2 = bLt$, where coefficient b is also a constant of order unity. Hence

$$\delta F_{tot} = \delta F_1 + \delta F_2 = \Delta\gamma(1 - aL^{1-p}) + bLt \tag{2}$$

The dependence on the thickness of the surface phase can be easily determined by minimizing δF_{tot} with respect to L, yielding the desired result: $L = t^{-1/p}$. In a typical system dominated by van der Waals-type forces,

$p = 3$, so L is expected to diverge algebraically with exponent $\nu = 1/p = 1/3$ [4]. As stated above, this analysis provides a convincing description of our experimental data.

Unlike the case of the SmA–HexB transition, long-range translational order is established both within and between the smectic layers through the SmA–CryB transition. Because enhanced surface ordering has now been observed in a number of liquid-crystal systems, it was not a complete surprise when surface transitions near the first-order SmA–CryB transition were also identified. Our recent calorimetric and optical reflectivity investigations have revealed up to six separate peaks associated with the SmA–CryB transition of 40.8 films (see Fig. 4). 40.8 refers to the liquid-crystal compound *n*-(4-*n*-butyloxybenzylidene)-4-*n*-octylaniline. The temperature dependence of the surface CryB penetration into the SmA substrate can again be well described by the power-law expression: $L = L_0((T_c(L) - T_c)/T_c)^{-\nu}$. Fitting yields the exponent $\nu = 0.36$. As in the SmA–HexB transition, this result is highly consistent with the standard wetting calculation, assuming that the interlayer interaction is van der Waals-like. This case is distinct, however, since it is the first layer-by-layer transition involving a liquid-crystal crystalline phase to be identified experimentally [12].

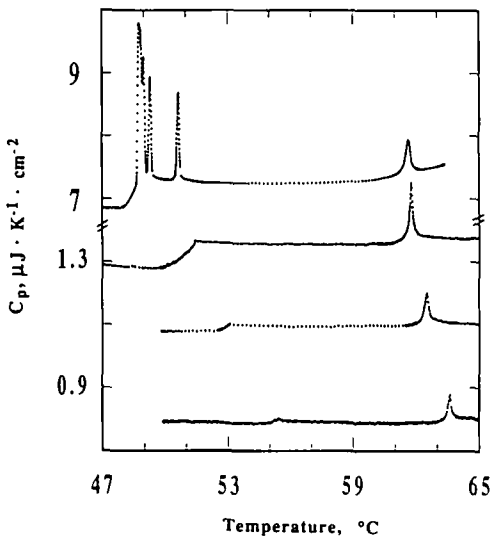

Fig. 4. Heat capacity as a function of temperature from 3-, 4-, 5-, and 25-layer films of 40.8 near the SmA–CryB transition. In the case of the 25-layer film, six separate heat-capacity peaks can be resolved.

Perhaps the most spectacular layer-by-layer transition exhibited by liquid crystals has been recently observed above the SmA–isotropic transition of H10F5MOPP [5-*n*-decyl-2-(4-*n*-perfluoropentylmetheleneoxy) phenyl)pyrimidine]. These molecules consist of a phenyl-pyrimidine core separating hydro-alkyl and fluoro-alkyl end chains. The perfluorination seems to have a profound impact on the behavior exhibited by this class of compounds. For example, the extremely low polarizability of the $-CF_2-$ and $-CF_3-$ groups may be expected to lead to a significant reduction in the van der Waals interaction along the molecular directors. The resulting relative promotion of the interaction perpendicular to the molecular director would enhance the tendency of these compounds to form smectic layers [13]. Not only are the smectic phase ranges greatly enhanced, but also the layer structure might be expected to be much more well developed in the perfluorinated analogues of the more common hydro-alkyl-terminated compounds. This observation becomes important in the discussion of the novel results obtained near the SmA–isotropic transition of H10F5MOPP.

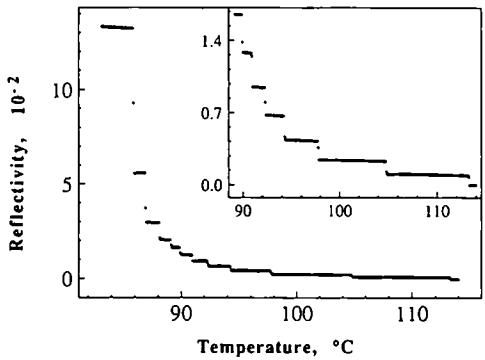

Fig. 5. Temperature variation of optical reflectivity above the bulk SmA–isotropic transition (85°C) of an initially 25-layer thick H10F5MOPP free-standing film. The layer thinning occurs as a series of discrete transitions in which interior layers become progressively disordered and drain out of the film to the film plate. From both heat capacity and optical reflectivity data, we determine that the thicknesses of the films corresponding to the sequence of plateaus are 25, 11, 9, 8, 7, 6, 5, 4, 3, and 2. The resulting thinning continues until the films become only two layers thick and eventually rupture near 113°C. The inset allows the reflectivity plateaus corresponding to two to eight layers to be more easily distinguished.

To date, when free-standing films of ordinary hydro-alkyl liquid–crystal compounds are heated, the films invariably rupture at or below the bulk isotropic transition temperature (T_{AI}). It was therefore quite surprising when H10F5MOPP films were observed to exhibit an extremely interesting layer-by-layer thinning transition well above the bulk T_{AI} [14]. Both our optical reflectivity (see Fig. 5) and heat capacity data indicate that the films thin as the interior layers become isotropic and are progressively squeezed out of the film by the van der Waals attraction between the films free surfaces. The temperature dependence of this effect is highly intriguing. If $T_{hc}(L)$ denotes the highest temperature at which a film of thickness L is stable, the film thickness is again found to obey the simple power law $L = L_0((T_{hc}(L) - T_{AI})/T_{AI})^{-\nu}$. However, in this case, the exponent obtained through the fitting was found to be $\nu \approx 3/4$. We know of no present theory that can adequately account for this observed behavior. This phenomenon is even more remarkable when one notes that two-layer SmA films remain stable more than 25 K above the bulk SmA–isotropic transition temperature (84°C). Evidently the enhanced intralayer coupling is strong enough to preserve the layer structure and prevent film rupture as interior layers drain into the surrounding reservoir of sample at the film plate edge.

In conclusion, we have presented and discussed three distinct liquid–crystal systems in which layer-by-layer transitions have been recently observed. The progression of both the SmA–HexB and the SmA–CryB transitions has been shown to be well described by a simple power law resulting from a standard wetting calculation assuming the interlayer interaction to be van der Waals-like. A similar power law has been found to describe the novel SmA–isotropic thinning transition recently discovered in perfluorinated liquid–crystal compounds. However, in this case, there does not appear to be any simple theory that can adequately account for the extremely large value of the exponent obtained.

ACKNOWLEDGMENTS

This work was supported in part by the National Science Foundation, Solid State Chemistry, Grant DMR93-00781. One of us (T.S.) would like to acknowledge support from IBM.

REFERENCES

1. T. Stoebe and C. C. Huang, *J. Modern Phys. B* (in press).
2. B. M. Ocko, A. Braslau, P. S. Pershan, J. Als-Nielson, and M. Deutsch, *Phys. Rev. Lett.* 57:94 (1986).

3. B. D. Swanson, H. Stragier, D. J. Tweet, and L. B. Sorensen, *Phys. Rev. Lett.* **62**:909 (1989).
4. A number of excellent review articles on wetting have been presented, including work by M. Schick, in *Liquids at Interfaces*, J. Charvolin, J. F. Joanny, and J. Zinn-Justin, eds. (Elsevier Science, Amsterdam, 1990), and P. G. de Gennes, *Rev. Mod. Phys.* **57**:827 (1985).
5. R. Geer, T. Stoebe, T. Pitchford, and C. C. Huang, *Rev. Sci. Instrum.* **62**:415 (1991).
6. T. Stoebe, C. C. Huang, and J. W. Goodby, *Phys. Rev. Lett.* **68**:2944 (1992).
7. T. Stoebe, R. Geer, C. C. Huang, and J. W. Goodby, *Phys. Rev. Lett.* **69**:2090 (1992).
8. R. Geer, T. Stoebe, and C. C. Huang, *Phys. Rev. E* **48**:408 (1993).
9. T. Stoebe, I. M. Jiang, S. N. Huang, A. J. Jin, and C. C. Huang, *Physica A* **205**:108 (1994).
10. D. J. Tweet, R. Holyst, B. D. Swanson, H. Stragier, and L. B. Sorensen, *Phys. Rev. Lett.* **65**:2157 (1990).
11. J. G. Dash, *Contemp. Phys.* **30**:89 (1989).
12. A. J. Jin, T. Stoebe, and C. C. Huang, *Phys. Rev. E* **49**:R4791 (1994).
13. E. P. Janulis, D. W. Osten, M. D. Radcliffe, J. C. Novack, M. Tristani-Kendra, K. A. Epstein, M. Keyes, G. C. Johnson, P. M. Savu, and T. D. Spawn, *SPIE-Int. Soc. Opt. Eng.* **1665**:143 (1992).
14. T. Stoebe, P. Mach, and C. C. Huang, *Phys. Rev. Lett.* **73**:1384 (1994).